

Chaos, fractals, and inflation

Neil J. Cornish

Department of Physics, Case Western Reserve University, Cleveland, Ohio 44106-7079

Janna J. Levin

Center for Particle Astrophysics, University of California at Berkeley, 301 Le Conte Hall, Berkeley, California 94720-7304

(Received 29 September 1995)

In order to draw out the essential behavior of the universe, investigations of early universe cosmology often reduce the complex system to a simple integrable system. Inflationary models are of this kind as they focus on simple scalar field scenarios with correspondingly simple dynamics. However, we can be assured that the universe is crowded with many interacting fields of which the inflaton is but one. As we describe, the nonlinear nature of these interactions can result in a complex, chaotic evolution of the universe. Here we illustrate how chaotic effects can arise even in basic models such as homogeneous, isotropic universes with two scalar fields. We find inflating universes which act as attractors in the space of initial conditions. These universes display chaotic transients in their early evolution. The chaotic character is reflected by the fractal border to the basin of attraction. The broader implications are likely to be felt in the process of reheating as well as in the nature of the cosmic background radiation.

PACS number(s): 98.80.Hw, 05.40.+j, 95.10.Fh, 98.80.Cq

I. INTRODUCTION

The inflationary paradigm strives to deliver a smooth universe from random initial conditions. If inflation is a robust attractor in the space of initial conditions, then it earns its claim to naturalness and genericity [1,2]. A universe which hosts many different fields, including an inflaton candidate, can develop an extreme sensitivity to initial values. This sensitivity marks the onset of chaos. Chaotic dynamics does not in itself destroy the robustness of an inflationary phase. Rather, it can lead to some powerful and perhaps observable implications for a realistic universe. For instance, a fractal pattern in the spectrum of density fluctuations could be generated. Also, the final phase of inflation marked by reheating would unavoidably be a setting for chaos.

In simple cosmologies, the ultimate fate of the universe can be predicted once a set of initial conditions is prescribed. In a closed cosmology, for instance, it can be determined from the initial prescription if the universe inflates or collapses. A plot in phase space will show regions or basins within which all of the initial conditions lead to the same outcome. There will be basins of inflation and basins of collapse. If the dynamics is *not* chaotic, these basins of attraction¹ are distinctly separated by smooth, regular boundaries. If the dynamics becomes chaotic, then the smooth boundaries begin to break up, ultimately becoming fractal.

The models described in the following sections are chosen on the grounds of simplicity, and do not necessarily conform to any standard inflationary scenario. In our current models the primary inflaton is weakly coupled and essentially not dynamical, leaving the chaotic dynamics to the other scalar

fields. Multiply coupled fields are quite natural in any particle theory. The Higgs field, for instance, must couple to the standard model fermions in order to induce fermion masses. In supersymmetric theories, a glut of coupled particles is expected. The fields behave effectively like nonlinearly coupled harmonic oscillators and so naturally bring on chaos. In future studies we intend to look at specific hybrid inflationary models [3] and draw out implications for the spectrum of fluctuations or the end of a realistic model. The main aim of this paper is to illustrate the complex dynamics that can arise in relatively simple cosmologies.

In addition to highlighting the appearance of chaos in inflationary cosmology, we aim to demonstrate the power of fractals as a quantitative measure of chaos in relativity. In general relativity coordinate-independent measures of chaos are of vital importance. One of the most valuable measures of a chaotic system in flat space, the Lyapunov exponents, can be removed by a simple coordinate transformation in curved space. Thus the usual coordinate-dependent measures of chaos become ambiguous in a relativistic context. Topological signals such as fractal basins, cantori, or stochastic layers in phase space are needed for conclusive evidence of chaos. In order to search for cantori or stochastic layers it is necessary to construct slices through phase space known as Poincaré sections. Since Poincaré sections rely on quasiperiodic behavior, the system must complete many cycles for a useful picture to emerge. Oftentimes relativistic systems are not so obliging as the evolution may end at singularities, such as the big crunch or inside a black hole. In these cases the dynamics is better suited to an outcomes-based approach such as the study of fractal basin boundaries [4].

In a chaotic system the different possible outcomes will each have a basin of attraction in the space of initial conditions, with the basins separated by a fractal border. A specific examination of phase space will require a coordinate system to be chosen. One might worry that in a different time slicing, the fractal would disappear. This is not possible. A co-

¹Throughout the paper we loosely refer to attractors in phase space. In more formal terminology, the word attractor is reserved for dissipative systems. Strictly speaking, our attractors are just asymptotic regions of phase space.

ordinate transformation must be smooth and differentiable. No smooth map can undo a truly fractal pattern as fractals are nondifferentiable. While the features of a fractal may be altered by a coordinate transformation, the existence of a fractal is unambiguous.

The cosmological context we employ allows us to demonstrate the technique of fractal basin boundaries. What emerges is a definitive manifestation of chaos in cosmology. We have already commented that we focus on multifield systems. If only one scalar field is present and the universe is closed, then there is still the possibility of chaotic regions in phase space [5–7]. However, in order to generate chaotic dynamics with just one matter field, the universe must oscillate between expansion and contraction many times. The requirement of many bounces makes these otherwise interesting solutions unlikely if not truly unphysical. We consider single-field scenarios in Sec. III. Since these bouncing candidates do not represent viable cosmologies, we turn our attention to many-field systems and the demonstration of fractal basin boundaries in Secs. IV and V. Also note that while we study closed cosmologies, the chaotic transients can be seen in a universe which never collapses or bounces. When fields interact, the chaotic nature is therefore not limited to closed cosmologies. It is thus possible that there was a transient chaotic epoch in the history of our own universe.

II. COSMOLOGICAL MODEL

In the coming examples we consider closed Friedmann-Robertson-Walker (FRW) universes. For potential-driven inflation to be successful the inflationary potential needs to be fairly constant. For our purposes the inflaton can be modeled by a simple cosmological constant. If this were the complete system, there would be of course no chaotic dynamics. However, the universe is created bursting with matter fields. We model the matter content by a variety of conformally and minimally coupled fields. These matter fields interact and can incite chaos. For the inflationary cases at hand, then, the chaotic behavior is principally matter driven, i.e., chaos in $T_{\mu\nu}$ causing chaotic evolution of $g_{\mu\nu}$.

The physical picture is that of a closed, preinflationary universe just exiting the Planck era. The space of initial conditions is probed by assigning three possible outcomes. Either the universe inflates forever, inflates for short spurts but then collapses, or collapses without any inflationary event. The outcome depends on the relative sizes of the various kinetic and potential energies in the matter fields. As the interaction between the matter fields is turned up the boundary which separates inflating from noninflating initial conditions blurs, eventually becoming fractal.

While we only consider closed models in our outcomes-based approach, the appearance of chaotic transients will be generic, regardless of curvature. This becomes clear since chaos is also nested within a given outcome basin. For instance, a universe will often go through rocky beginnings, enduring many fits of inflation before taking off smoothly or collapsing. Within a collapse basin, the sensitivity to the initial conditions shows up as a random scatter in the maximum radius of the universe or in the final value of the fields. If the universe has managed to inflate by several e -folds, there is no turning back as the kinetic energy which might interrupt

inflation quickly redshifts away. This feature of the de Sitter attractor is often referred to as cosmic baldness. We shall see that while the de Sitter attractor might end up bald, it can have very hairy beginnings.

We shall consider FRW universes described by the metric

$$\begin{aligned} ds^2 &= dt^2 - a^2 \left(\frac{dr^2}{1-kr^2} - r^2 d\Omega^2 \right) \\ &= a^2 \left(d\tau^2 - \frac{dr^2}{1-kr^2} - r^2 d\Omega^2 \right), \end{aligned} \quad (1)$$

where t is cosmic time and τ is conformal time. Throughout, overdots will denote derivatives with respect to cosmic time and primes will denote derivatives with respect to conformal time. The matter Lagrangian will contain various combinations of conformally, Ψ , and minimally, Φ , coupled scalar fields with a variety of interaction terms described by the potential $V(\Psi, \Phi)$:

$$\mathcal{L}_M = V - \frac{1}{2} \partial_\mu \Phi \partial^\mu \Phi - \frac{1}{2} \partial_\mu \Psi \partial^\mu \Psi + \frac{1}{12} \mathcal{R} \Psi^2. \quad (2)$$

For comparison with the conformally coupled term, i.e., the last term in Eq. (2), the gravitational Lagrangian is $\mathcal{L}_G = -\frac{1}{12} \mathcal{R}$. We have chosen units where $4\pi G/3 = c = 1$. In terms of cosmic time t the field equations read

$$\ddot{\Phi} + 3H\dot{\Phi} + \partial_\Phi V = 0, \quad (3)$$

$$\ddot{\Psi} + 3H\dot{\Psi} + \partial_\Psi V + \frac{\mathcal{R}}{6} \Psi = 0, \quad (4)$$

$$\ddot{a} + a \left(2\dot{\Phi}^2 + (\dot{\Psi} + H\Psi)^2 + \frac{k}{a^2} \Psi^2 + \Psi \partial_\Psi V - 2V \right) = 0. \quad (5)$$

The Ricci scalar can be related to the scale factor through $\mathcal{R}/6 = \ddot{a}/a + H^2 + k/a^2$. The Hubble expansion factor is given by $H = \dot{a}/a$. The total energy of the system is

$$\mathcal{H} = H^2 + \frac{k}{a^2} - \dot{\Phi}^2 - (\dot{\Psi} + H\Psi)^2 - \frac{k}{a^2} \Psi^2 - 2V = 0. \quad (6)$$

The constraint, Eq. (6), can be obtained directly from Einstein's field equations and represents the first integral of Eq. (5).

Since we are dealing with the entire universe, the system is necessarily conservative. We use Eq. (6) to ensure that energy is in fact conserved. It is amusing to notice that if we isolate the matter sector, this subsystem looks dissipative. Energy is lost to the gravitational field through the friction terms $\sim 3H\dot{\Phi}$. We can see the effects of dissipation within the larger context of the Hamiltonian system. For instance we can watch the matter trajectories shrink down onto an attractor as the volume in phase space is dissipated (cf. Sec. V).

In some cases it is profitable to recast the field equations in terms of conformal time τ , and the rescaled variables $\psi = a\Psi$, $\phi = a\Phi$, and $U = a^4 V$:

$$\phi'' - \frac{a''}{a}\phi + \partial_\phi U = 0, \quad (7)$$

$$\psi'' + k\psi + \partial_\psi U = 0, \quad (8)$$

$$a'' + ka + \frac{1}{a}\left(\phi' - \frac{a'}{a}\phi\right)^2 - \frac{1}{a}(4U - \psi\partial_\psi U) = 0. \quad (9)$$

The total energy of the system can be expressed as

$$\begin{aligned} a^4 \mathcal{H} &= (a')^2 + ka^2 - \left(\phi' - \frac{a'}{a}\phi\right)^2 - [(\psi')^2 + k\psi^2] - 2U \\ &= 0. \end{aligned} \quad (10)$$

A universe is said to inflate if the scale factor a accelerates in terms of cosmic time, i.e., $\ddot{a} > 0$. The cosmic time acceleration is given by

$$\begin{aligned} \ddot{a} &= \frac{aa'' - (a')^2}{a^3} \\ &= \frac{1}{a^3} \left[2U - \psi\partial_\psi U - (\psi')^2 - k\psi^2 - 2\left(\phi' - \frac{a'}{a}\phi\right)^2 \right]. \end{aligned} \quad (11)$$

Notice that conformally coupled fields tend not to contribute to a positive acceleration. In other words, even with a potential $\propto \Psi^n$, conformally coupled fields do not drive inflation (unless $n < 2$). The generalization of the above equations to describe two or more scalar fields of either type is direct.

The field equations are invariant under the combined rescaling

$$a \rightarrow xa, \quad t \rightarrow xt, \quad V \rightarrow \frac{V}{x^2}, \quad (12)$$

where x is a constant. This freedom is removed when we set our length scale by choosing dimensionful values for quantities such as masses and coupling constants.

As we describe below, the asymptotic solutions are of two kinds. The universe eventually approaches a smooth de Sitter phase or it ultimately collapses into a big crunch. In highly simplified models the division between these two outcomes can be expressed as a simple partition in the space of initial conditions. However, we shall see that even in simple models with two interacting fields the division is no longer clean, as the boundaries separating the different outcomes are no longer smooth curves but fractals.

A. From integrability to chaos

When the various scalar fields are massless and do not interact the equations of motion can be integrated exactly and there is no chaos. Before launching into the chaotic dynamics, we take a look in this subsection at the two asymptotic possibilities, the big crunch and de Sitter expansion, which will be the basis of our outcomes-based approach in the following sections. We also show the phase space portraits for the noninteracting, closed system. In Ref. [1], a detailed analysis was given of the phase space portraits for a single, massive, minimally coupled field in a universe with

arbitrary curvature. According to their portraits, the trajectories drawn are untangled and therefore are not chaotic. As the authors noted, there does exist a set of measure zero oscillatory solutions which do show chaotic behavior [5]. At the close of Sec. III we return to discuss this special set of perpetually bouncing solutions.

For now we demonstrate the nonchaotic phase space for a universe full of noninteracting, garden variety fields (both minimally and conformally coupled). Since it is impossible to tell one scalar field from another in the absence of interactions, the general case of N minimally coupled and M conformally coupled scalar fields reduces to a universe with one field of each type. For a universe with a scalar field of each type and cosmological constant Λ the equations simplify to

$$\psi = A \cos \tau, \quad (13)$$

$$\left(\frac{\phi}{a}\right)' = \frac{B}{a^2}, \quad (14)$$

$$a' = \pm \sqrt{A^2 + 2a^4\Lambda + \frac{B^2}{a^2} - a^2}. \quad (15)$$

The phase space is divided by a separatrix into two classes of trajectories, those that terminate at the big crunch and those that inflate. The form of the solutions can easily be found in the neighborhood of these two geometrically distinct attractors. When the dynamics is dominated by potential terms, such as a cosmological constant Λ , the universe undergoes exponential expansion and matter fields are redshifted away:

$$a \sim e^{\sqrt{2\Lambda}t} \sim -\left(\frac{1}{\sqrt{2\Lambda}\tau}\right), \quad \phi \sim a^{-2}, \quad \psi \sim \cos \tau. \quad (16)$$

Conversely, when the dynamics is dominated by the kinetic energy of the matter fields or spatial curvature, the universe collapses to the big crunch at time τ_c :

$$a \sim |\tau - \tau_c|^{1/2}, \quad \phi \sim a \ln a, \quad \psi \sim \cos \tau, \quad (17)$$

for $B \neq 0$, and for $B = 0$,

$$a \sim |\tau - \tau_c|, \quad \phi \sim \text{const}, \quad \psi \sim \cos \tau. \quad (18)$$

The separatrix that partitions these possibilities is defined by the trajectory with

$$\Lambda = \frac{A^2 + 2\sqrt{A^4 + 3B^2}}{6(A^2 + \sqrt{A^4 + 3B^2})^2}. \quad (19)$$

For these simple, integrable cosmologies the basins of attraction for the big crunch and de Sitter attractors are separated by a smooth curve. This smooth curve is a portion of the separatrix. In Fig. 1 we display phase space portraits in the (a, a') and (ψ, ψ') planes for a universe with $B = 0$ and $\Lambda = 1/8$. The crosshatched region is the basin of the big crunch attractor and the solid line is the separatrix.

When interactions are included the separatrix breaks up and is replaced by a fractal curve. The gaps in the broken separatrix have the structure of a Cantor set. The broken

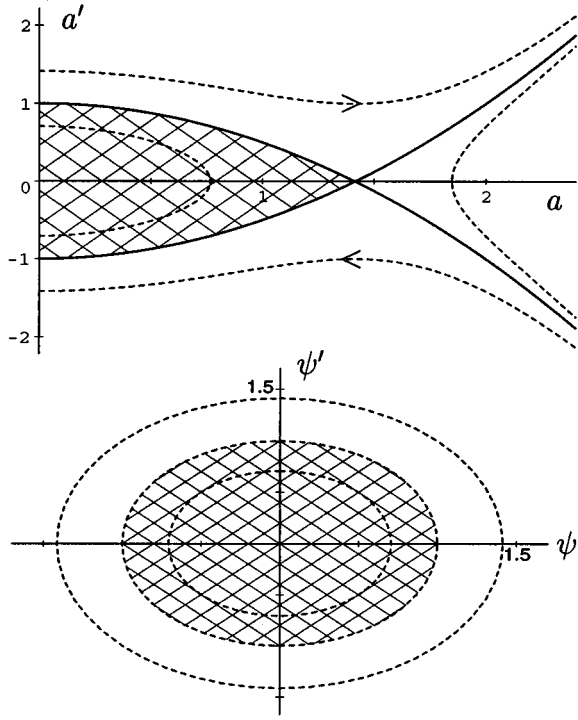


FIG. 1. Phase space trajectories in the (a, a') and (ψ, ψ') planes for universes with noninteracting scalar fields. The solid line is the separatrix and the crosshatched regions mark the big crunch basin of attraction.

separatrix no longer partitions phase space and trajectories may diffuse through it. For example, a universe that was destined to collapse in the integrable case might diffuse through the broken barrier and inflate. The breaking of the separatrix is reflected in the fractal nature of the basin boundaries for chaotic universes. The smooth basin boundaries shown in Fig. 1 should be compared to the fractal boundaries seen in Figs. 4 and 7, below. The break up of the separatrix is further described in Sec. IV.

Even when interactions are included, the asymptotic behavior of trajectories on either attractor is completely regular and nonchaotic. Examples of this fact are given in Sec. V. In the parlance of dynamical systems theory, the attractors are neither strange nor chaotic. The chaotic behavior is transient [8], and occurs when trajectories approach the broken separatrix. Physically this corresponds to an epoch in which the universe coasts with a fairly constant radius but with wildly varying acceleration. During this epoch the kinetic and potential energies in the system fight for supremacy and the universe teeters between collapse and violent expansion. If the kinetic energy dominates, the universe collapses and the asymptotic solution can be found by neglecting all potential terms in the equations of motion. Conversely, if the potential energy dominates, the asymptotic solution can be found by neglecting kinetic energy terms.

The transient nature of the chaos is similar to that found in the mixmaster universe [9,10], where it has been shown that the underlying attractors are neither strange nor chaotic [11]. We remark that transient chaos appears to be the hallmark of relativistic systems.

III. COSMOLOGIES WITH A SINGLE SCALAR FIELD

Since we work with a closed FRW cosmology, there is only one parameter describing the gravitational sector, namely, the scale factor. The necessary elements for chaos are present if the scale factor interacts even with just one matter field. However, the dynamical time scale for the onset of chaos is longer than the life of one universe. The chaotic dynamics results as the two oscillators interact. Typically, at least a few oscillations are needed for the effects to surface. We discuss such an example in this section. On the other hand, if there are many interacting matter fields in the universe, then their chaotic evolution will make an impact during the lifetime of one universe. The examples of the following section reveal chaos on such short time scales.

We begin with an example that is chaotic, but only on a time scale longer than the life of one universe. The model describes a single, conformally coupled scalar field in a closed ($k=1$) universe. We choose the potential to have both a mass term and a cosmological constant Λ :

$$U = \frac{1}{2} m^2 a^2 \psi^2 + a^4 \Lambda. \quad (20)$$

This example has previously been considered by Calzetta and El Hasi [6,7]. The Hamiltonian takes the form

$$a^4 \mathcal{H} = (a')^2 + a^2 - [(\psi')^2 + \psi^2 + m^2 a^2 \psi^2] - 2a^4 \Lambda = 0, \quad (21)$$

which, aside from the wrong sign for the gravitational contributions, is the Hamiltonian for two coupled harmonic oscillators.

For a metric with only one dynamical degree of freedom it is always possible to perform a combined field redefinition and conformal transformation to a coordinate system in which the dynamics appears to be nonsingular. By using conformal rather than cosmic time to describe the evolution of this system, the dynamical equations can be smoothly integrated past the big bang and big crunch singularities at $a=0$. This allows many cosmic cycles to be considered if we continue the scale factor into negative values. When evolved through a series of cosmic cycles the system is clearly chaotic [6,7], as we might expect for nonlinearly coupled oscillators. It should be noted that the cosmic cycles are physically meaningless as all memory of the previous cycle is erased at each big crunch singularity.

By introducing the fiction of cosmic cycles, the dynamics can be surveyed using the standard tools of Poincaré sections (return maps) and Lyapunov exponents. Lyapunov exponents measure the rate of separation of trajectories in phase space. Only if trajectories separate exponentially fast do they have positive exponents. Systems with positive Lyapunov exponents are said to exhibit sensitive dependence on initial conditions, one of the two ingredients of chaos (the other being the mixing and folding of trajectories). The inverse of the positive Lyapunov exponents is referred to as the Lyapunov time scale. This time scale sets the dynamical time scale over which chaotic effects make themselves felt. In general relativity, Lyapunov exponents must be used with extreme care, if at all, as they are coordinate dependent. Indeed, a simple

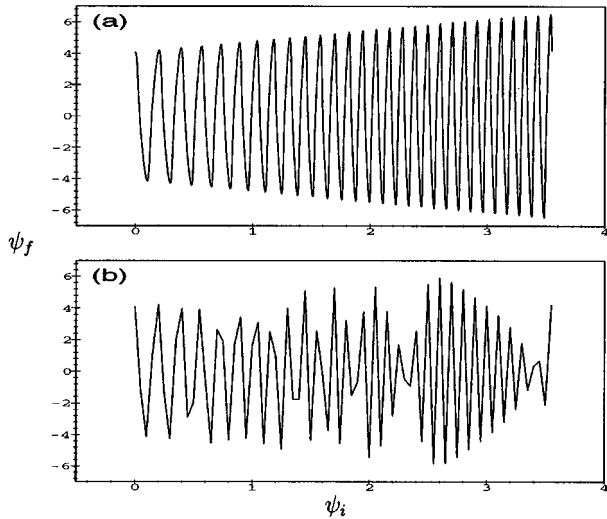


FIG. 2. The correlation between initial and final values of the scalar field (a) is compared to the apparently chaotic behavior seen in (b) where the sampling rate is 10 times lower.

coordinate transformation can give a nonchaotic system positive exponents and a chaotic system vanishing exponents.

Putting these reservations aside, we may compare the Lyapunov time to the time taken to complete a cosmic cycle, and infer whether or not chaotic effects can make themselves felt in the lifetime of a single universe. Typically, the Lyapunov time scale was found to be in the range $10 \rightarrow 1000$ cosmic cycles. Even when the mass is taken to be very large, the Lyapunov time scale is always found to be greater than half a cosmic cycle, or in other words, the time scale for chaos to become important always exceeds the life of one universe. This result is easily understood. The chaotic behavior is due to resonances between the two oscillating fields a and ψ . In order for the resonance to take effect, both fields typically need to oscillate several times. However, a can only complete half an oscillation before the big crunch, making it exceedingly difficult for a chaotic resonance to occur.

In Ref. [6] it was argued that chaos had been viewed within the span of one life cycle. Their conclusion was based on what appeared to be a scatter between initial values of the matter fields and the final values. The correlation between initial and final values of the scalar field ψ was found to be 0.01. However, this low value for the correlation actually stems from a coarse sampling of a high frequency function. By regenerating Fig. 6 of Ref. [6] with a sampling rate that is 10 times higher we see from Fig. 2 that the true correlation coefficient is 1.00. This confirms that the system shows no meaningful chaotic effects in the life of one universe.

Similar conclusions hold for universes inhabited by a single minimally coupled scalar field. Again, the equations of motion can lead to chaotic behavior as they are nonlinear and have phase space dimension greater than 2. However, meaningful chaotic effects can only occur if the universe itself oscillates. The dynamics of an inflationary model driven by a minimally coupled scalar field with the potential

$$V = \frac{1}{2} m^2 \Phi^2 + \frac{\lambda}{4} (\Phi^2 - \Phi_0^2)^2 \quad (22)$$

was studied by Belinskii *et al.* [1], and with $\lambda = 0$ by Hawking [12] and Page [5]. Typical trajectories were not chaotic. Rather, they see the universe smoothly evolve from the big bang to the big crunch with various amounts of inflation [1]. However, the inflationary potential allows some atypical trajectories for which the universe undergoes a number of non-singular bounces [12]. Page [5] suggested that there exists an uncountably infinite but discrete set of perpetually bouncing universes with vanishing Lebesgue measure but nonvanishing fractal dimension. If Page's suggestion is correct, it would prove that the dynamics is chaotic as his "fractal set of perpetually bouncing universes" corresponds to what is now known as a strange repeller [13]. In contrast to the fictional cosmic cycles used to describe a conformally coupled scalar field, Page's bouncing universes are true, nonsingular solutions. However, these solutions have obvious drawbacks as plausible cosmologies. As remarked in Ref. [1], the fine-tuning required to arrive at these chaotic trajectories rules them out as a robust physical model displaying chaotic behavior. Perhaps in a model of the early universe that generically displays nonsingular bounces we can hope to see interesting chaotic effects caused by an oscillating scale factor [14]. In the absence of such a model we have to look to additional matter fields to provide the nonlinear resonances needed to incite chaos.

IV. COSMOLOGIES WITH TWO CONFORMALLY COUPLED FIELDS

If additional fields occupy the universe, then the scale factor will not be the principle source of chaos. Two scalar fields can oscillate many times in the lifetime of one universe, leading to truly chaotic behavior. To demonstrate the chaos we show the fractal basin boundaries for a universe which contains two conformally coupled fields which interact through the potential

$$U = \frac{1}{2} m_1^2 a^2 \psi_1^2 + \frac{1}{2} m_2^2 a^2 \psi_2^2 + \lambda^2 \psi_1^2 \psi_2^2 + a^4 \Lambda. \quad (23)$$

The period of oscillation for each field is governed by its effective mass. We define the reduced effective mass for each field as the derivative with respect to the field of the field, Eq. (9). In other words, M_ψ^2 has the form of $\partial^2 W / \partial \psi^2$ where W is anything which acts as a potential in the equations of motion:

$$M_a = (1 - m_1^2 \psi_1^2 - m_2^2 \psi_2^2 - 4\Lambda a^2)^{1/2}, \quad (24)$$

$$M_1 = (1 + m_1^2 a^2 + 2\lambda^2 \psi_2^2)^{1/2}, \quad (25)$$

$$M_2 = (1 + m_2^2 a^2 + 2\lambda^2 \psi_1^2)^{1/2}. \quad (26)$$

Increasing m_1 , m_2 , Λ , and λ slows the recollapse of a and speeds the oscillation of ψ_1 and ψ_2 , thus increasing the probability of chaotic resonances. However, if m_1 or m_2 greatly exceeds λ , the resonances will be washed out and no chaos will be seen. Conversely, if m_1 and m_2 are both zero, the oscillations tend to freeze when ψ_1 and ψ_2 hit small values, again making chaotic resonances unlikely.

To gain some intuition we can find a simple analytic approximation which corresponds to a familiar chaotic system. During the majority of the universe's evolution, the scale

factor varies much more slowly than the scalar fields so that $a'/a \ll \psi'_i/\psi_i$. The scalar fields behave like coupled nonlinear oscillators, adiabatically pumped by the slowly varying scale factor. To leading order we can ignore the adiabatic pumping all together and study the scalar field dynamics in a fixed background ($a' \approx 0$). This approximation is particularly good for describing universes that are vacillating between collapse and inflationary expansion. Importantly, this is just the region where the chaotic transients occur that destroy the smooth separatrix of the integrable model described in Sec. II A. When $a' \approx 0$ the dynamics simplifies to that of two coupled oscillators:

$$\psi_1'' + \omega_1^2 \psi_1 + 2\lambda^2 \psi_2^2 \psi_1 = 0, \quad (27)$$

$$\psi_2'' + \omega_2^2 \psi_2 + 2\lambda^2 \psi_1^2 \psi_2 = 0, \quad (28)$$

where $\omega_i^2 = 1 + m_i^2 a^2$ is the fixed frequency of the uncoupled ($\lambda = 0$) oscillators. The above system of equations describes a known chaotic system [15], and the transition to chaos as λ is increased can be studied using the Chirikov resonance overlap condition [16]. Having established that the fast variables ψ_1 and ψ_2 behave chaotically, we can then consider how they back react on the slow variable a . When looked at on time scales long compared to the periods of the scalar fields, the evolution of the scale factor is similar to Brownian motion, and can be described in terms of chaotic diffusion equations [8]. It is this buffeting of the scale factor by the matter fields that breaks the separatrix in the (a, a') plane and causes the universe to evolve in a chaotic manner.

Returning to the full, unapproximated equations we numerically investigate the phase space of initial conditions. For a given set of initial conditions we can identify three main outcomes. The first possibility sees the universe expand and collapse without any inflationary burst. The second possibility sees the universe undergo one or many short bursts of inflation, but failing to become a macroscopic universe. The third possibility sees the universe sustain a prolonged and violent period of inflation, resulting in the formation of a macroscopic universe. The first and second possibilities (colored black and grey, respectively) combine to form the big crunch basin of attraction. This artificial division of the big crunch basin is mostly for visual effect. There is a fourth possible outcome that should be mentioned. There is a set of trajectories with zero Lebesgue measure that oscillate eternally, never entirely collapsing, nor reaching the de Sitter attractor. These trajectories form the border between the big crunch and de Sitter basins of attraction. We will see that these trajectories belong to a fractal set of perpetually bouncing universes. In the parlance of dynamical systems theory, this set forms the stable manifold of a strange repeller [8].

The three possibilities are displayed graphically in Fig. 3 for the choice of parameters ($\Lambda = 0.0001, m_1 = 0, m_2 = 0.05, \lambda = 1$) and initial conditions $\{a(0) = 2, \psi_1 = 0.4, \psi_2 = 6, \psi_2' = 20\}$. The initial values of ψ_1' are $\{-23.31, -23.32, -23.33\}$, and $a'(0)$ is fixed by the Hamiltonian constraint.

The fact that minute changes in the initial conditions can lead to such dramatic changes in the outcome suggests that the fate of our model universe is indeed chaotic. This suspicion can be confirmed by studying the boundary between the basins of attraction of the three outcomes. Since the basins

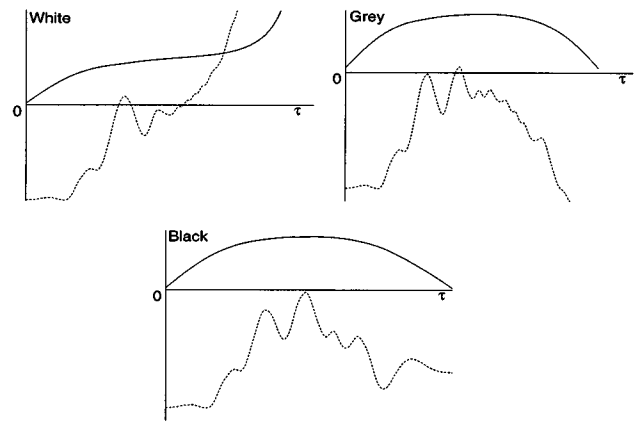


FIG. 3. The three possible outcomes for the universe. In each case the solid line is the scale factor a and the dashed line is the scaled acceleration $\ddot{a}a^3$. The initial values for ψ_1' are -23.31 , -23.32 , and -23.33 , respectively.

are embedded in a six-dimensional phase space, we are forced to consider lower dimensional slices through the boundary. In Fig. 4 we display a two-dimensional slice in the $\psi_1 - \psi_1'$ plane for universes with parameters and conditions identical to those used in Fig. 3. The three basins of attraction (black, grey, white) are dramatically intermixed *strange basins*, as at least a portion of the boundaries is fractal. The boundaries near the origin are regular and smooth while the outer boundaries appear fragmented. A detail of the outer region is shown in Fig. 5, visually confirming the fractal nature of the boundary. Repeated magnification reveals similar striated pictures on all scales.

Rather than rely on these qualitative features, we may quantify the fractal nature of the boundary in terms of the fractal dimension. There are many definitions of fractal dimension that we may choose from, but the one best suited to our situation is the box counting dimension. On a two-dimensional slice through phase space we cover the fractal

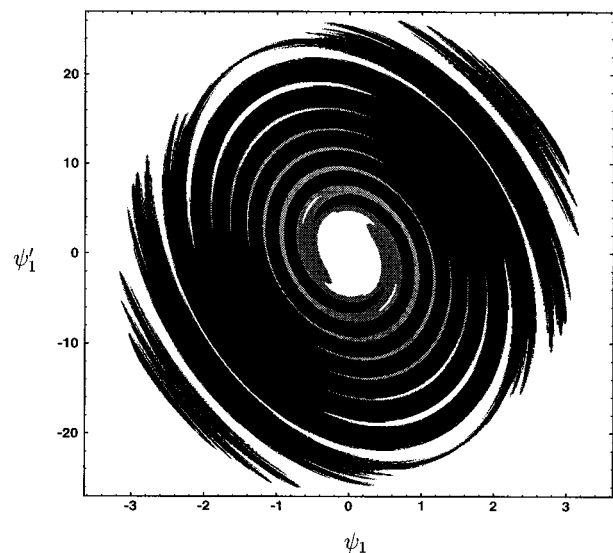


FIG. 4. The basins of attraction for universes similar to those shown in Fig. 3.

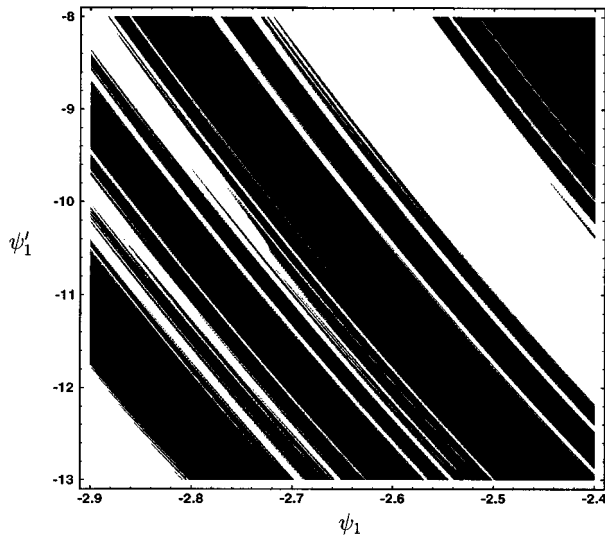


FIG. 5. A detail of Fig. 4.

with a grid of squares with side length ε . We then count the number $N(\varepsilon)$ of squares needed to cover the fractal, i.e., the number of squares containing more than one color. The box dimension d_B is defined by

$$d_B = - \lim_{\varepsilon \rightarrow 0} \frac{\ln N}{\ln \varepsilon}. \quad (29)$$

For self-similar structures the formal limit $\varepsilon \rightarrow 0$ need not be taken, and in all practical situations we are only interested in the existence of such scaling laws over a large, but not necessarily infinite, range of scales. Since the fractal dimension is not invariant under homeomorphisms, it is not a true topological invariant. However, it is invariant under diffeomorphisms, and so it does provide a topological measure in general relativity. *The existence of fractal structures in phase space provides a coordinate-independent signal of chaos in relativity.*

The importance of the fractal dimension of the basin boundaries can be described in terms of final state sensitivity [17]. Consider an initial configuration near the basin boundary, where the uncertainty in the initial conditions describes an N -dimensional ball of radius δ in the N -dimensional phase space. The final state sensitivity f_δ is the fraction of phase space volume which has an uncertain outcome due to the uncertainty in the initial conditions, and is given by

$$f_\delta = \delta^\alpha, \quad \alpha = N - d_B. \quad (30)$$

For a nonchaotic system $\alpha = 1$ and the final state sensitivity is directly proportional to the initial uncertainty. For chaotic systems, however, $0 < \alpha < 1$, and the uncertainty in the outcome is greater than the uncertainty in the initial conditions. For example, if $\alpha = 0.47$, a 50% reduction in the initial uncertainty only reduces the final state uncertainty by 28%. In this way, the dimension of the basin boundary is a direct measure of the ‘‘sensitive dependence on initial conditions.’’

In Fig. 6 we display the plot used to determine the fractal dimension of Fig. 5. Because the three boundaries are densely interwoven in this case, we chose only to calculate the dimension of the boundary between the big crunch and

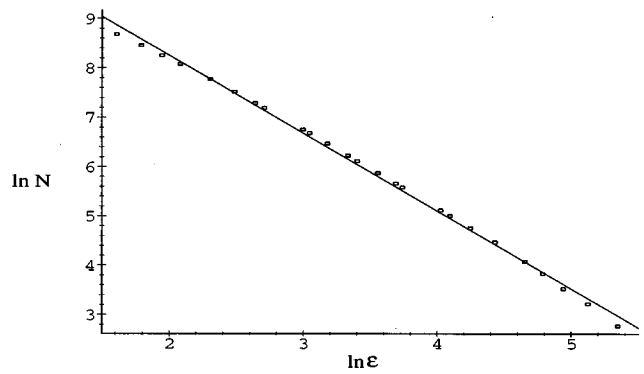


FIG. 6. Finding the fractal dimension for Fig. 5. The solid line is a least-squares fit to the box counting data. The dimension was found to be $d_B = 1.58 \pm 0.02$.

de Sitter attractors, i.e., counting grey and black as one basin. Using an 840×840 grid we found the dimension to be 1.58 ± 0.02 . The grid size of $840 = 2^3 \times 3 \times 5 \times 7$ was chosen as it has the most factors of any number below 1000. The curvature of the data points at small and large ε is to be expected. For large ε the covering is very inefficient, while for small ε the squares saturate the resolution used to generate the fractal. These effects cause d_B to tilt toward 2 for large ε and toward 1 for small ε . Despite these limitations, accurate fractal dimensions can be obtained very quickly and easily. For different choices of parameters we found fractal dimensions ranging from 1 to 1.96, essentially filling the allowed range $d_B = [1, 2]$.

The boundary was found to be fractal on all possible two-dimensional slices. For example, in Fig. 7, the boundary is shown in the a - a' plane for a slice which intersects Fig. 4 along the line $\psi_1 = 1.0$. The fractal dimension of this slice was found to be $d_B = 1.37 \pm 0.02$.

While the previous chaotic pictures were typical of those found, the dynamics of the system is not always chaotic. For small values of λ, m_1, m_2 (at fixed scaling x) the dynamics is

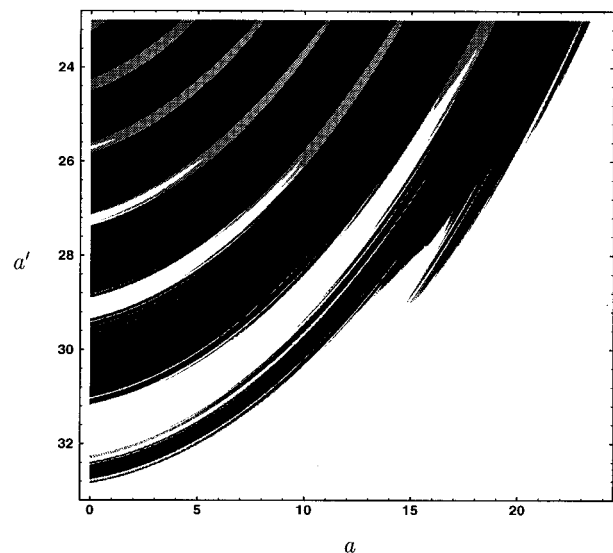


FIG. 7. A slice in the a - a' plane which intersects the ψ_1 - ψ_1' plane of Fig. 4 along the line $\psi_1 = 1.0$.

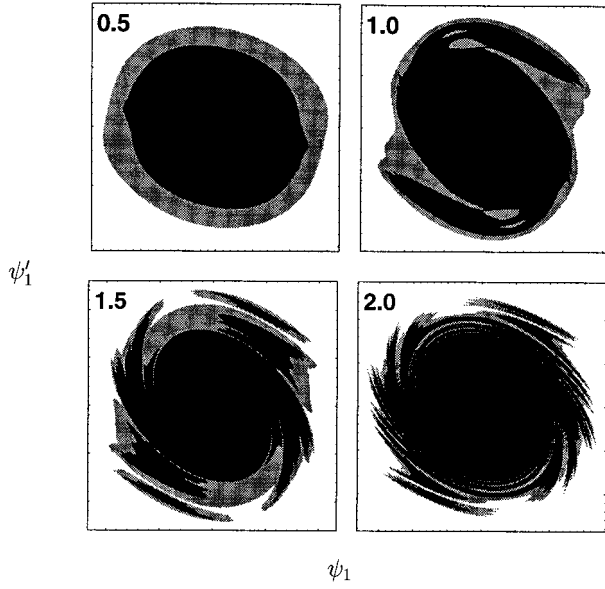


FIG. 8. The road to chaos: As λ is incremented from 0.5 to 2.0, the nonlinear distortion of the attractor basin mounts. Once λ exceeds 1.0 the mixing is so strong that the boundaries become fractured and, eventually, fractal. The graphs were generated for the choice of parameters and initial conditions $\Lambda = 0.000\,02$, $a_0 = 10$, $\psi_2 = 5.0$, $\psi_2' = 10.0$, $m_1 = 0.2$, $m_2 = 0.1$.

near integrable and the basins are not strange, but regular. In Fig. 8 we increment λ while keeping all other parameters and initial conditions fixed. The mixing of the basins is reminiscent of the blending of viscous fluids. The dimension of the basin boundary for $\lambda = 0.5$ was found to be $d_B = 0.99 \pm 0.02$, which is consistent with a dimension of 1. So, within errors, this boundary is smooth and nonchaotic. To compare, the dimensions of the boundaries for $\lambda = 2.0$ were $d_B = 1.16 \pm 0.05$ (grey-white) and $d_B = 1.26 \pm 0.05$ (grey-black).

An important property of dynamical systems with strange attractor basins is that the chaotic dynamics is not restricted to phase space trajectories near the fractal boundaries. One way to see this might be to use the fiction of cosmic cycles to follow the evolution of trajectories starting in the big crunch basin. The Lyapunov exponents and Poincaré sections for

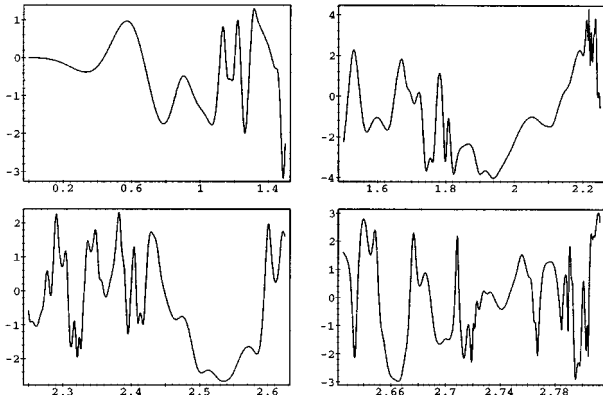


FIG. 9. The correlation between ψ_{1i} (vertical axis) and ψ_{1m} (horizontal axis) on a $\psi_1' = 0$ slice through the big crunch basin of attraction of Fig. 8 ($\lambda = 2.0$).

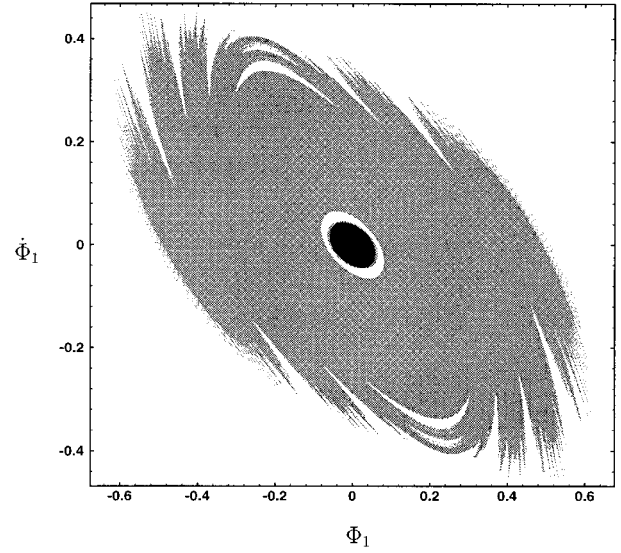


FIG. 10. Basins of attraction in the Φ_1 - $\dot{\Phi}_1$ plane for universes containing two minimally coupled scalar fields.

these trajectories would reveal chaotic behavior across the basin. However, we are not really interested in effects which take longer than one universe's lifetime to make themselves felt. Instead we plot in Fig. 9 the correlation between the initial value of ψ_{1i} and the value at the point of maximum expansion, ψ_{1m} . The graphs are for a $\psi_1' = 0$ slice through the big crunch basin of Fig. 8 with $\lambda = 2.0$. The big crunch basin stretches from $\psi_1 = 0$ to $\psi_1 \sim 2.9$ (and similarly for negative ψ_1). A general increase in frequency with increasing ψ_{1i} requires that we use several plots, each covering half the region of the last, to cover the basin. Unlike the regular plot seen in Fig. 2, the relationship between initial and final values of ψ_1 is highly erratic, with apparently random changes in frequency and amplitude.

V. COSMOLOGIES WITH MINIMALLY AND CONFORMALLY COUPLED FIELDS

The chaotic behavior seen in the previous system is not restricted to conformally coupled fields. Similar behavior is found for minimally coupled fields with the same choice of potential. The main difference in this case comes from the scalar fields themselves being a source of inflation, in addition to the cosmological constant. The acceleration in this example is given by

$$\ddot{a} = 2a \left(\Lambda + \frac{1}{2} m_1^2 \Phi_1^2 + \frac{1}{2} m_2^2 \Phi_2^2 + \lambda^2 \Phi_1^2 \Phi_2^2 - \dot{\Phi}_1^2 - \dot{\Phi}_2^2 \right), \quad (31)$$

where we have reverted to the unscaled field variables. These models are able to successfully inflate even when there is no cosmological constant, in a manner similar to Linde's "chaotic inflation" [18]. However, we did not see any strange basins when $\Lambda = 0$ as successful inflation generally required the fields to become stuck high up in their potentials after just a few oscillations. Otherwise, their ability to climb high enough was lost due to friction and redshifting of kinetic energy. It may be that chaotic behavior does occur when

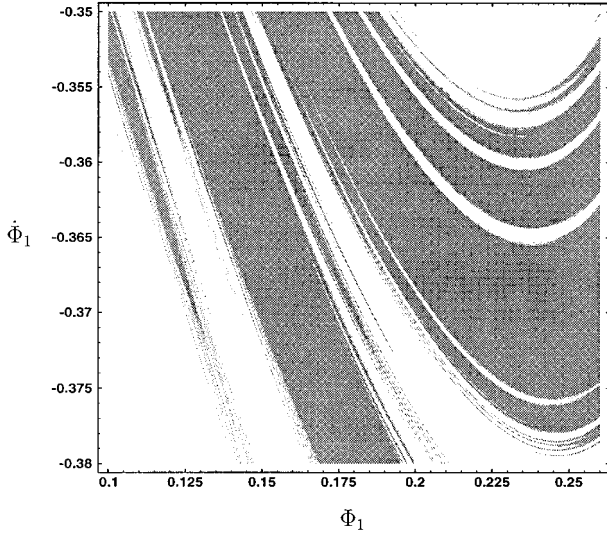


FIG. 11. A detail of Fig. 10 where the dimension is $d_B = 1.54 \pm 0.02$.

$\Lambda = 0$, but it is difficult to search for as the inflationary bursts must be followed for ~ 60 e -folds in comparison to the $\sim 5-10$ e -folds required to ensure we have reached the de Sitter attractor when $\Lambda \neq 0$.

In Fig. 10 we display the basins of attraction in the Φ_1 - $\dot{\Phi}_1$ plane for universes with $(m_1=0, m_2=0.04, \Lambda=0.00005, \lambda=1.0)$ and fixed initial conditions $\{a(0)=10.0, \Phi_2=0.4, \dot{\Phi}_2=0.16\}$. A detail of the outer boundary is shown in Fig. 11, where the dimension was found to be 1.54 ± 0.02 . Because the scalar fields themselves contribute to the inflationary bursts, there is typically far more of the grey basin than we saw for conformally coupled fields.

We can compare an analysis of the chaotic trajectories with the nonchaotic trajectories of Sec. II A. While the universe is expanding ($H > 0$), we see from Eq. (3) that the scalar field dynamics is effectively that of a damped harmonic oscillator. Conversely, as the universe contracts the dynamics is that of a pumped harmonic oscillator. This behavior is apparent in Fig. 12, where we have displayed typical trajectories leading to the de Sitter and big crunch attractors. For the de Sitter attractor the scalar fields spiral into a fixed point as cosmic baldness asserts itself, while for the big crunch attractor the scalar fields first spiral in and then spiral out again as the universe collapses. The de Sitter attractor has an interesting structure when two fields are present as one scalar field gets locked at a constant value. The attractor is of the form

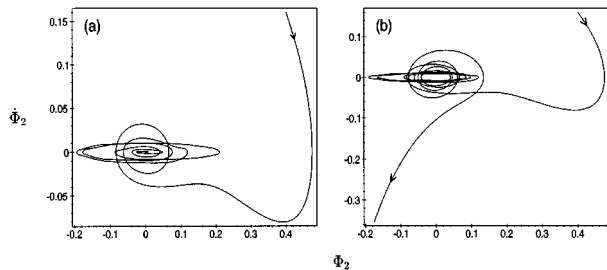


FIG. 12. (a) A trajectory spiraling into the de Sitter attractor. (b) A nearby trajectory which flows out to the big crunch attractor.

$$a = a_c \exp(\sqrt{2\Lambda}t), \quad (32)$$

$$\Phi_2 = \Phi_{2c} \exp\left(-\frac{3\sqrt{2\Lambda}}{2}t\right) \cos \omega t, \quad (33)$$

$$\Phi_1 = \Phi_{1c} \left[1 + \lambda^2 \Phi_{2c}^2 \exp(-3\sqrt{2\Lambda}t) \left(\frac{t}{3\sqrt{2\Lambda}} + \frac{2\omega \cos^2 \omega t + 3\sqrt{2\Lambda} \cos \omega t \sin \omega t}{2\omega(9\Lambda + 2\omega^2)} \right) \right], \quad (34)$$

subject to the restriction

$$\omega^2 = m_2^2 + 2\lambda^2 \Phi_{1c}^2 - \frac{9}{2}\Lambda. \quad (35)$$

For reference, the trajectory in Fig. 12(a) has $\Phi_{1c} = 0.00573$, $\Phi_{2c} = 105.9$, and $\omega = 0.03796$. The big crunch attractor is unchanged from the one-field case, and takes the form

$$a = a_c (t_c - t)^{1/3}, \quad (36)$$

$$\Phi_1 \sim \Phi_{1c} \ln(t_c - t), \quad (37)$$

$$\Phi_2 \sim \Phi_{2c} \ln(t_c - t), \quad (38)$$

with $\Phi_{1c}^2 + \Phi_{2c}^2 = 1/9$. The trajectory shown in Fig. 12(b) has $t_c = 200.004$, $a_c = 13.68$, $\Phi_{1c} = 0.294$, and $\Phi_{2c} = 0.167$. Since we are able to write down analytic solutions for trajectories on the attractors, it is clear that the de Sitter and big crunch attractors are nonchaotic. The chaotic behavior seen during the evolution of the universe is restricted to the $5 \rightarrow 10$ transient orbits seen in Fig. 12. The fractal nature of the attractor basin boundaries is due entirely to these brief chaotic transients.

We close with a word on a mixed cosmology which contains one minimally coupled and one conformally coupled scalar field. The conformally coupled scalar field Ψ is taken to be massless. When Ψ 's coupling to the minimally coupled scalar field Φ is small it behaves like radiation. The interaction potential is taken to be

$$V = \frac{1}{2}m^2\Phi^2 + \lambda^2\Psi^2\Phi^2 + \Lambda. \quad (39)$$

As before, the minimally coupled scalar field is able to contribute a negative pressure to that of the inflaton, thereby increasing the likelihood of inflationary bursts. Again, this increases the proportion of grey over what we saw for two conformally coupled fields.

By viewing the basins in the a - \dot{a} plane we see some rather striking ink-blot and crystal boundaries. An example of this is shown in Fig. 13 for the choice of parameters $(m=0.05, \Lambda=0.0001, \lambda=2)$ and fixed initial conditions $\{\Phi=0.2, \Psi=0.1, \dot{\Psi}=0.08\}$. A detail of the grey-white crystal boundary is shown in Fig. 14. The high degree of self-similarity of this fractal allowed a particularly accurate determination of the fractal dimension using a standard 840×840 grid. The dimension was found to be

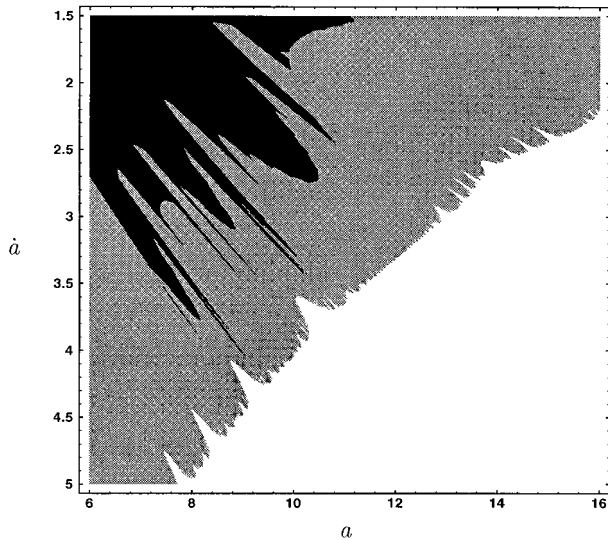


FIG. 13. The basins of attraction in the a - \dot{a} plane for universes containing a minimally coupled scalar field and a massless, conformally coupled scalar field.

$d_B = 1.484 \pm 0.005$. The visually less fractal grey-black ink-blot boundary was found to have a smaller fractal dimension of $d_B = 1.11 \pm 0.05$, with the larger error due to a lower degree of self-similarity.

In addition to studying different combinations of minimally and conformally coupled scalar fields, we also considered a variety of polynomial potentials $V(\Phi, \Psi)$. The qualitative results were the same for all cases, showing that chaotic evolution was a generic feature of all multifield models.

VI. DISCUSSION

The early universe is likely to contain many interacting fields. We have shown that if these interactions are sufficiently strong, the evolution of the universe will be chaotic. The fractal basin boundaries reveal the chaos in a coordinate-

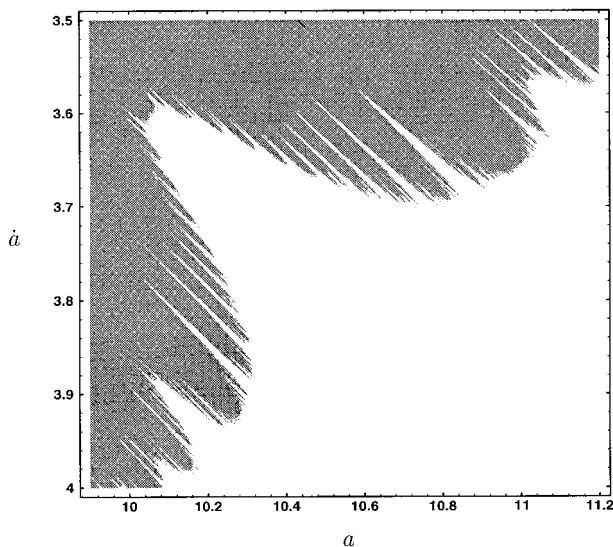


FIG. 14. A detail of Fig. 13 where the dimension is $d_B = 1.484 \pm 0.005$.

independent manner. Additionally, the method does not require one universe to pass through many cycles. We now have to ask how prevalent chaotic behavior will be in particular models of inflation, and what implications it might have for processes such as reheating or galaxy formation.

One model of inflation where chaotic dynamics is bound to be important is hybrid inflation. Hybrid models employ several interacting scalar fields, and arise naturally in various supersymmetric theories where the breaking of large gauge groups employs many Higgs particles [19]. If in the early stages the universe inflates in jolts, an exciting possibility exists for the spectrum of primordial density fluctuations. Chaotic resonances could lead to a fractal power distribution, perhaps helping to explain the hierarchical clustering seen in the current universe. Moreover, chaotic evolution of the scale factor would leave a unique imprint on the gravitational waves produced during inflation [20]. Any chaotic behavior would have to occur within the last ~ 60 e -folds of inflation to be observable today. This would require some artificial fine-tuning in a single-field model but may be more natural in a hybrid model.

Even in inflationary models where chaotic evolution is unimportant at early stages, chaos is sure to play an important role at the end stages. To illustrate, consider again a hybrid model. The fields to which the inflaton couples dictate the occurrence of the true vacuum and so control the nature of the exit from inflation. The setting is prime for chaotic interactions which would certainly impact on the exit style. More generically, at the end of any inflation model, the universe reheats as the inflaton oscillates about the minimum of its potential. Particles are thereby produced through the inflaton's coupling to other matter fields. If the matter fields are dynamical and chaos reigns, then the process of entropy production would deserve rethinking. The importance of parametric resonances, which are closely related to chaotic behavior, has already been stressed in this context [21,22].

It seems appropriate to consider how chaotic dynamics might impact on "chaotic" inflation [18]. In chaotic inflation different patches of the universe are taken to have different values of the inflaton and matter fields. In some patch, it is argued, the inflaton is sufficiently high up in the potential and the matter fields are sufficiently small so as to permit a long-lived inflationary epoch [2]. For initial field values deep within a basin, away from the fractal borders, the usual arguments hold and the chaotic inflation paradigm is largely unaffected. However, if in a given patch the field values are near a fractal basin boundary, it can become difficult to find a patch of any size across which the conditions are regular enough to allow this thinking. Even the slightest variation in the initial conditions across the patch will lead to an entirely different outcome. Because of the self-similar nature of the fractal, no matter how small you try to make the patch, there will still be slight variations in the conditions and hence the outcome. For cosmological conditions in the vicinity of the fractal basin boundary, then, the simple FRW thinking must be abandoned.

For similar reasons, caution would be needed for slow-roll initial conditions as well. In fact the slow-roll scenario will likely be more fragile as the inflaton is more easily kicked around. For chaotic initial conditions by contrast the

inflaton is high up in its potential and thus resilient against the influence of kicks and bumps.

Aside from direct observational effects there are also some important theoretical implications raised by chaotic evolution. For example, chaotic systems are characterized by an entropy, the Kolmogorov-Sinai entropy, which is related to the spectrum of Lyapunov exponents. This introduces a chaotic arrow of time in addition to the cosmological and thermodynamic arrows of time. As well, it raises the question of a possible connection between the Kolmogorov-Sinai entropy and the thermodynamic entropy released at the end of inflation. Another issue raised by chaotic dynamics concerns the recovery of a semiclassical limit in quantum cosmology due to the breakdown of the WKB approximation in chaotic systems [23].

We have suggested a few implications for chaotic dynamics in largely unexplored terrain. Chaos theory grew out of

Poincaré's study of the solar system, and with its development came insights into the intricate structures of our neighborhood such as the asteroid belt and Saturn's rings. It seems fitting for chaos to have an impact not only on the evolution of the solar system but also on the birth of the universe. We are left to ask if chaotic fingerprints have been left on the large-scale landscape as they were on the landscape of our own solar system.

ACKNOWLEDGMENTS

We have enjoyed discussions with Matt Holman and Jihad Touma. We thank John Barrow, Norm Frankel, Andrei Linde, and Don Page for their helpful comments. We are indebted to Carl Dettmann for making his original programs available to us, and to Jacques Legare for his help in making modifica-

-
- [1] V. A. Belinskii, L. P. Grishchuk, I. M. Khalatnikov, and Ya. B. Zel'dovich, *Phys. Lett.* **155B**, 232 (1985); *Sov. Phys. JETP* **62**, 195 (1985).
 - [2] D. S. Goldwirth and T. Piran, *Phys. Rep.* **214**, 223 (1992); *Phys. Rev. D* **40**, 3263 (1989); A. D. Linde, *Phys. Lett.* **162B**, 281 (1985); R. H. Brandenberger and J. H. Kung, *Phys. Rev. D* **42**, 1008 (1990).
 - [3] A. D. Linde, *Phys. Lett. B* **259**, 38 (1991); *Phys. Rev. D* **49**, 748 (1994).
 - [4] C. P. Dettmann, N. E. Frankel, and N. J. Cornish, *Phys. Rev. D* **50**, R618 (1994); *Fractals* **3**, 161 (1995).
 - [5] D. N. Page, *Class. Quantum Grav.* **1**, 417 (1984).
 - [6] E. Calzetta and C. El Hasi, *Class. Quantum Grav.* **10**, 1825 (1993).
 - [7] E. Calzetta and C. El Hasi, *Phys. Rev. D* **51**, 2713 (1995).
 - [8] E. Ott, *Chaos in Dynamical Systems* (Cambridge University Press, Cambridge, England, 1993).
 - [9] C. Misner, *Astrophys. J.* **151**, 431 (1968).
 - [10] J. D. Barrow, *Phys. Rep.* **85**, 1 (1982).
 - [11] P. Ma and J. Wainwright, in *Deterministic Chaos in General Relativity*, edited by A. Burd, A. Coley, and D. Hobill (Plenum, New York, 1994), p. 449.
 - [12] S. W. Hawking, in *Relativity Groups and Topology II*, Proceedings of the Les Houches Summer School, Les Houches, France, 1983, edited by R. Stora and B. S. De Witt, *Les Houches Summer School Proceedings Vol. 40* (North-Holland, Amsterdam, 1984).
 - [13] L. P. Kadanoff and C. Tang, *Proc. Natl. Acad. Sci. USA* **81**, 1276 (1984); H. Kantz and P. Grassberger, *Physica D* **17**, 75 (1985).
 - [14] J. D. Barrow and M. P. Dabrowski, *Mon. Not. R. Astron. Soc.* **275**, 850 (1995).
 - [15] B. V. Chirkov and D. L. Shepelyansky, *JETP Lett.* **34**, 163 (1981); G. K. Savvidy, *Phys. Lett.* **130B**, 303 (1983); G. Contopoulos, H. E. Kandrup, and D. Kaufmann, *Physica D* **64**, 310 (1993).
 - [16] B. V. Chirikov, *Phys. Rep.* **52**, 265 (1979).
 - [17] C. Grebogi, S. McDonald, E. Ott, and J. Yorke, *Phys. Lett.* **99A**, 415 (1983).
 - [18] A. D. Linde, *Phys. Lett.* **129B**, 177 (1983).
 - [19] A. Guth, L. Randall, and M. Soljatic, MIT Report No. MIT-CTP-2499 (unpublished).
 - [20] L. P. Grishchuk and M. Solokhin, *Phys. Rev. D* **43**, 2566 (1991).
 - [21] L. Kofman, A. D. Linde, and A. A. Starobinsky, *Phys. Rev. Lett.* **73**, 3195 (1994).
 - [22] Y. Shtanov, J. Traschen, and R. H. Brandenberger, *Phys. Rev. D* **51**, 5438 (1995).
 - [23] M. V. Berry, in *Chaotic Behaviour of Deterministic Systems*, proceedings of the Les Houches Summer School of Theoretical Physics, Les Houches, 1981, edited by G. Ios, R. Helleman, and R. Stora (North-Holland, Amsterdam, 1983), Session 36.